IEEE Access
Multidisciplinary ⁝ Rapid Review ⁝ Open Access Journal

Received May 15, 2020, accepted June 21, 2020, date of publication June 26, 2020, date of current version August 20, 2020.

Digital Object Identifier 10.1109/ACCESS.2020.3005344

Improved Energy Balance Control for Boost Converters Without Estimating Circuit Energy Losses

LEI WANG, (Member, IEEE), QINGHUA WU, AND WENHU TANG, (Senior Member, IEEE)

School of Electric Power Engineering, South China University of Technology (SCUT), Guangzhou 510641, China

Corresponding author: Wenhu Tang (wenhutang@scut.edu.cn)

This work was supported in part by the State Key Program of National Natural Science Foundation of China under Grant U1866210, and in part by the Project funded by China Postdoctoral Science Foundation under Grant 2019M662910.

ABSTRACT The previously developed control methods based on the conservation of energy in circuits require the accurate estimation of energy losses, which is difficult to measure and calculate for boost converters. Consequently, there always exist steady-state errors in the output voltage if neglecting such circuit energy losses. To address this issue, an improved energy balance control (IEBC) method is proposed in this paper by integrating a simplified energy balance controller (SEBC) with a PI controller. The proposed IEBC can reduce the steady-state output voltage errors without requiring the estimation of circuit energy losses. Furthermore, the proposed IEBC can operate in both the continuous current mode (CCM) and the discontinuous current mode (DCM), thus accurate static and fast dynamic performances are achieved over the entire load operation range. Moreover, the stability of the IEBC is proved using the Lyapunov stability criterion. Compared with that of the SEBC, both simulations and experiments validate the feasibility and robustness of the proposed IEBC method.

INDEX TERMS Boost converter, energy balance, steady-state error, dynamic performance.

I. INTRODUCTION

With the expanding of power converters applications, the requirement for the performance of power converters has become increasingly high, for instance, small size, light weight, high efficiency and so on. In this case, the conventional PID controller, although having the advantages of simple control principle and strong robustness, cannot fulfil the rising requirements of converters, e.g., fast dynamic response [1], [2]. Then an anti-windup PI controller has been proposed. By switching between the saturation and linear regions, improved dynamic response was implemented to the load variation. However, a switch condition first have to determine and there is no significant improvement on the input variations or disturbances [3], [4]. Recently, to get superior static and dynamic performances, various control methods were developed, such as hysteresis control, sliding-mode control, fuzzy control, etc [5]–[10]. As an attempt to obtain excellent performances, the law of energy conservation, which states that the total amount of energy in a system is constant, has been introduced into the control field. It was firstly introduced to control the rigid body of active magnetic bearings, which provided a new view on the closed loop control [11]. Up to now, the application areas based on such a principle covered stability control of power systems, hamiltonian system, photovoltaic systems, active power filters, converters and so on [12]–[16].

As for converter applications, the conservation of energy was introduced to obtain the reference current and voltage of converters in a hybrid control scheme [17], [18], then improved dynamic performances were achieved. However, this scheme is only suitable for the critical discontinuous current mode (CDCM) and the discontinuous current mode (DCM). Under the continuous current mode (CCM), it is difficult to obtain a reference current, since not all the energy absorbed by an inductor can be released in full at the end of one switching cycle. A controller covering entire load operating ranges was presented in [19], [20] based on the law of energy conservation. Simulation results of a buck converter illustrate that it is not vulnerable to changes of converter operation modes (CCM, CDCM, DCM) and can offer fast dynamic performances. A switching control scheme (SCS)

The associate editor coordinating the review of this manuscript and approving it for publication was Fuhui Zhou.

using the law of energy conservation was presented for controlling buck converters [21]. By considering the energy losses of a circuit when maintaining the energy conservation in the circuit, the SCS achieved accurate static and fast dynamic performances. Similarly, by considering the energy losses of the circuit, accurate static and fast dynamic performances were achieved based on the energy balance in boost converters [22]. However, the mathematical calculation of energy losses in a circuit is complex. Moreover, parasitic parameters of circuit components are usually unknown and difficult to be measured in actual circuits, which leads to the inaccurate estimation of such energy losses. Thus the energy losses in a circuit are usually neglected, as a result, leading to degraded performance, mainly the steady-state errors of the output voltage. To reflect this phenomenon, according to the previously developed control methods using the circuit energy conservation, a simplified energy balance control (SEBC) method, which neglect energy losses of circuits, is firstly derived in this paper. Then combined with a voltage PI controller, an IEBC method is proposed to tackle the degraded performance caused by neglecting circuit energy losses.

The main contents of the paper are as follows: Using the SEBC method, Section II analyses the steady-state errors to the output voltage caused by neglecting circuit energy losses; Section III designs and implements the proposed IEBC method; The stability of the IEBC boost converter is analyzed in Section IV; Section V discusses simulation and experimental results; Conclusion is given in Section VI.

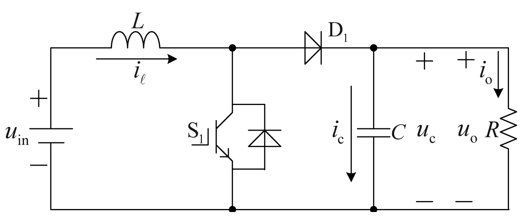

FIGURE 1. The circuit structure of a boost converter.

II. THE ANALYSIS OF THE SEBC

FIGURE. 1 shows the circuit structure of a boost converter, where i_ℓ denotes the inductor current, i_o represents the load current, u_c represents the capacitor voltage and u_o represents the output voltage. Under the assumption $u_c = u_o = u_{ref}$, the conservation of energy in a boost converter is expressed as (1) [18], [19]. Defining T_s as a switching cycle duration, at the beginning of the n^{th} switching cycle, S_1 is turned on by a clock pulse with a fixed frequency, and the DC source injects energy into the circuit. As time goes on, the energy that the DC source injects into the circuit increases by integration and is compared with the sum of the consumed energy of load $(u_{ref} - u_{in})i_o T_s$, the stored energy of the inductor $\int_{(n-1)T_s}^{(n-1)T_s+T_s} u_\ell i_\ell dt$ and the circuit energy losses, mainly due to the parasitic DC resistance R_ℓ of the inductor $\int_{(n-1)T_s}^{(n-1)T_s+T_s} i_\ell^2 R_\ell dt$. At the instant when the output of the integrator reaches the control reference, S_1 is turned off. S_1 remains off until the next clock pulse arrives. Thus the control methods based on the conservation of energy in the circuit keeps the output voltage to a desired value.

It should be noted that, the variables u_{in}, i_ℓ, i_o of (1) are not the functions of time t but sampled and updated at the beginning of every sampling period T_c, which is the time point kT_c. And these variables are regarded as constants, since the duration of a sampling period is short. Due to its complicated measurement and computation, the circuit energy losses, mainly $\int_{(n-1)T_s}^{(n-1)T_s+T_s} i_\ell^2 R_\ell dt$ of (1) produced by the parasitic DC resistance R_ℓ of the inductor, is usually neglected. As a result, (2) represents the control equation of SEBC.

III. THE DERIVATION OF CONTROL EQUATION AND IMPLEMENTATION OF THE PROPOSED IEBC

A. THE CONTROL EQUATION DERIVATION OF THE IEBC

It is generally known that a PI controller attempts to minimize the error over time by adjusting the control variable $u(t)$ so as to force a measured process variable $y(t)$ to follow a desired value $r(t)$. It means that the merit of the PI controller is to eliminate the errors between a control objective and a controlled object, and as a result, the PI controller relies only on the response of the measured process variable, not on the exact mathematical model. In consideration of such features of PI controller, a voltage PI controller is introduced to modify the SEBC method for eliminating the steady-state errors of the output voltage Δu_{steady} due to neglecting the energy losses of the circuit. To implement the PI voltage controller, the following changes are made to equation (2) of SEBC.

Firstly, the converter is emulated by an equivalent resistance R_e shown in Fig. 2, thus i_ℓ is expressed as

$$i_\ell = \frac{u_{in}}{R_e}. \quad (3)$$

$$\int_{(n-1)T_s}^{(n-1)T_s+t_{on}(n)} u_{in} i_\ell dt = (u_{ref} - u_{in}) i_o T_s + \int_{(n-1)T_s}^{(n-1)T_s+T_s} u_\ell i_\ell dt + \int_{(n-1)T_s}^{(n-1)T_s+T_s} i_\ell^2 R_\ell dt \quad (1)$$

$$\int_{(n-1)T_s}^{(n-1)T_s+t_{on}(n)} u_{in} i_\ell dt = (u_{ref} - u_{in}) i_o T_s + u_\ell i_\ell T_s \quad (2)$$

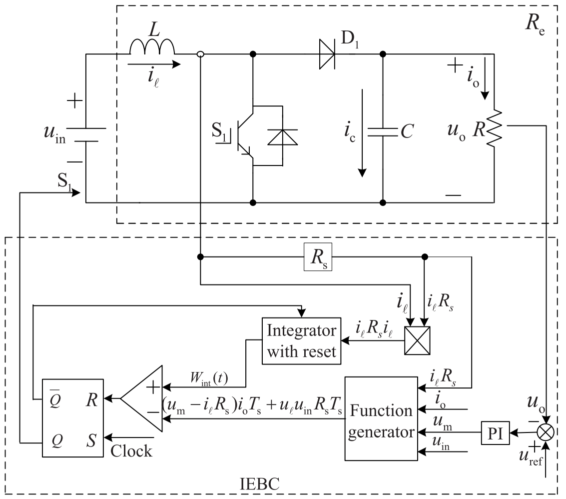

FIGURE 2. The diagram of the proposed IEBC for boost converters.

Based on (3), the following equation can be deduced,

$$R_e = \frac{u_{in}}{i_\ell}. \tag{4}$$

Multiplying both sides of (2) by $\frac{R_e}{R_s}$, (5) is derived from (2). Based on (3) and (4), (5) is changed into (6), where $u_m = \frac{u_{ref}}{R_e}R_s$, which is obtained from the PI voltage controller [23], as shown in FIGURE 2. The proportional term K_p of the PI voltage controller is designed to be high enough, so that the dynamic response is not slowed down.

Thus, the control equation of the proposed IEBC method is derived as (6). With the high robustness of the PI controller, the steady-state errors of the output voltage due to the neglection of circuit energy losses can be eliminated.

B. THE IMPLEMENTION OF THE IEBC

As shown in FIGURE 2, the implementation of the IEBC method is described as below. The control reference $(u_m - i_\ell R_s)i_o T_s + \frac{u_\ell i_\ell^2 R_s T_s}{u_{in}}$ is calculated instantaneously, which is calculated at the beginning of every sampling period and kept as the same during the entire sampling period. After getting the control reference, the proposed IEBC method is implemented by integration and comparison. The implementation of a CCM boost converter using the proposed IEBC method is described as below: the integral begins in the time instant when S_1 is turned on by a clock pulse with a fixed frequency. Over time, the integral W_{int} keeps increasing from its initial value as follows:

$$W_{int}(t) = \int_{(n-1)T_s}^{(n-1)T_s+t_{on}(n)} i_s^2 R_s dt \quad (t \in ((n-1)T_s, (n-1)T_s + T_s]) \tag{7}$$

and W_{int} is constanly compared with the control reference. At the moment when $W_{int}(t)$ reaches to the control reference, a reset pulse is generated by the comparator in FIGURE 2 to reset the RS flip-flop as $Q = 0$, which turns off S_1. In the meantime, the integral is reset. S_1 keeps as the off-state until the next clock pulse arrives, then the $(n+1)^{th}$ switching cycle starts. Since a DCM boost converter has the similar implementation procedures with that of CCM, it is not presented in detail here.

IV. STABILITY ANALYSIS OF THE IEBC BOOST CONVERTER

Under the steady-state conditions, the inductor absorbs and releases equal energy, which means $W_\ell(t) = 0$. Thus, neglecting W_ℓ, (6) is rewritten as follows:

$$\int_{(n-1)T_s}^{(n-1)T_s+t_{on}(n)} i_\ell^2 R_s dt = (u_m - i_\ell R_s) i_o T_s \tag{8}$$

Then the average model of (8) is obtained as:

$$i_\ell^2 R_s d = (u_m - i_\ell R_s) i_o \tag{9}$$

From (9), d can be derived as:

$$d = \frac{(u_m - i_\ell R_s) i_o}{i_\ell^2 R_s} \tag{10}$$

And such a boost converter can be described as:

$$\begin{aligned} \frac{di}{dt} &= \frac{u_{in}}{L} - \frac{1-s}{L}u, \\ \frac{du}{dt} &= -\frac{u}{RC} + \frac{1-s}{C}i \end{aligned} \tag{11}$$

where $s = 1$ represents the on-state of switch S_1, $s = 0$ represents the off-state of switch S_1.

Substituting s in (11) with the value of d derived above, the state-space averaged model of the energy balance controlled

$$\begin{aligned} &\frac{R_s}{R_e}\int_{(n-1)T_s}^{(n-1)T_s+t_{on}(n)} u_{in} i_\ell dt = \frac{R_s}{R_e}(u_{ref} - u_{in}) i_o T_s + \frac{R_s}{R_e} u_\ell i_\ell T_s \\ \Longrightarrow &\int_{(n-1)T_s}^{(n-1)T_s+t_{on}(n)} \frac{u_{in}}{R_e} i_\ell R_s dt = (\frac{u_{ref}}{R_e}R_s - \frac{u_{in}}{R_e}R_s) i_o T_s + \frac{R_s}{R_e} u_\ell i_\ell T_s \end{aligned} \tag{5}$$

$$\int_{(n-1)T_s}^{(n-1)T_s+t_{on}(n)} i_\ell^2 R_s dt = (u_m - i_\ell R_s) i_o T_s + \frac{u_\ell i_\ell^2 R_s T_s}{u_{in}} \tag{6}$$

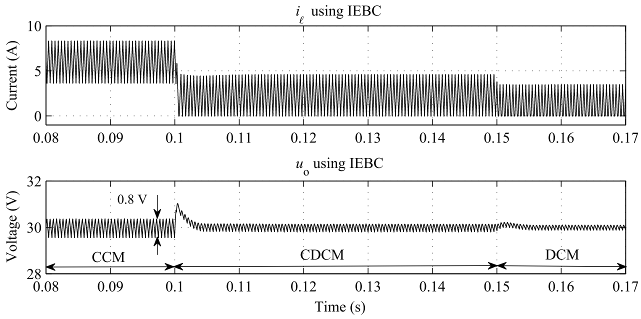

FIGURE 3. The simulation results using the IEBC of the boost converter operating in the entire load range (10 Ω → 27 Ω → 47 Ω).

boost converter is obtained as follows.

$$\frac{di}{dt} = \frac{u_{in}}{L} - \frac{u}{L}[1 - \frac{(u_m - i_\ell R_s)i_o}{i_\ell^2 R_s}],$$
$$\frac{du}{dt} = -\frac{u}{RC} - \frac{i}{C}[1 - \frac{(u_m - i_\ell R_s)i_o}{i_\ell^2 R_s}] \quad (12)$$

Let the values of $\frac{di}{dt}$ and $\frac{du}{dt}$ in (12) equal to 0, then the equilibrium point is obtained as follows:

$$V = \frac{u_m^2 u_{in}}{u_s^2 R},$$
$$I = \frac{u_m u_{in}}{u_s} \quad (13)$$

The Jacobian matrix evaluated at this equilibrium point is derived as follows

$$J = \begin{pmatrix} -\frac{v^2(u_m - u_s)}{Lu_s RI^2} & -\frac{1}{L} + \frac{2(u_m - u_s)V}{u_s IRL} \\ \frac{1}{C} & -\frac{1}{RC} - \frac{(u_m - u_s)}{Cu_s R} \end{pmatrix} \quad (14)$$

Substituting (13) into the jacobian matrix gets

$$J = \begin{pmatrix} -\frac{(u_m - u_s)u_s R}{Lu_m^2} & \frac{u_m - 2u_s}{Lu_m} \\ \frac{1}{C} & -\frac{u_m}{Cu_s R} \end{pmatrix} \quad (15)$$

By solving the characteristic equation $det[\lambda I - J] = 0$, the following characteristic quasi-polynomial equation is obtained:

$$f(\lambda) = (\lambda + \frac{(u_m - u_s)u_s R}{Lu_m^2})(\lambda + \frac{u_m}{Cu_s R}) - \frac{u_m - 2u_s}{LCu_m}$$
$$= \lambda^2 + [\frac{(u_m - u_s)u_s R}{Lu_m^2} + \frac{u_m}{CRu_s}]\lambda + \frac{u_s}{LCu_m} \quad (16)$$

By performing a second-order Pad approximation, (16) can be written as follows:

$$a_2\lambda^2 + a_1\lambda + a_0 \quad (17)$$

where $a_2 = 1$, $a_1 = \frac{(u_m - u_s)u_s R}{Lu_m^2} + \frac{u_m}{CRu_s}$ and $a_0 = \frac{u_s}{LCu_m}$.

It is clear that $a_2 > 0$. Since $u_m = \frac{u_{ref}}{R_e} R_s$, $u_m > 0$ and $(u_m - u_s) > 0$ by combining with (4), thus $a_1 > 0$ and $a_0 > 0$ are obtained, which satisfies the Routh−Hurwitz criterion. Hence, the IEBC is stable.

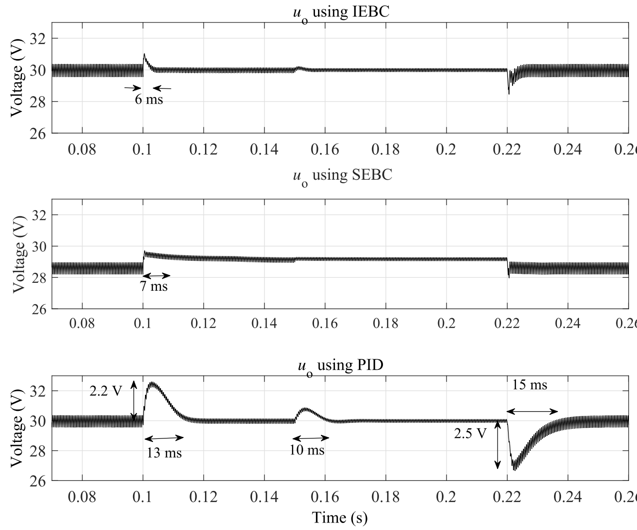

FIGURE 4. The responses of u_o to load steps (10 Ω → 27 Ω → 47 Ω → 10 Ω).

V. SIMULATION AND EXPERIMENTAL RESULTS

Simulation and experimental results are used to demonstrate the superior performances of the IEBC. And a current-mode PID controller and the SEBC method are built for comparative study. The parameters of the boost converters designed in this research are as follows: $u_{in} = 15$ V, $u_{ref} = 30$ V, $f_s = 2$ kHz, $L = 800$ μH, $C = 1000$ μF, $R = 10$ Ω. The sample time is $T_c = 10\,\mu s$. The boost converters are designed for the case of a low-voltage high-current application using a lower switching frequency. In such a case, the steady-state errors, due to the neglection of energy losses, are more severe.

A. SIMULATION COMPARISON RESULTS

FIGURES 3 illustrate the simulation results of the boost converter using the IEBC in the entire operation range. From the figure, it is observed that the IEBC is capable of operating stably in the entire operation range (CCM, CDCM and DCM).

① At $t = 0$, the system starts operation with $R = 10$ Ω and $u_{in} = 15$ V. As shown in FIGURES 3, the converter operates in CCM and u_o settles at the pre-set value 30 V with ripples limited within 0.8 V.

② At $t = 0.1$ s, the load is stepped to 27 Ω abruptly. The converter changes its operation mode from CCM to CDCM. u_o jumps to 30.8 V due to such a sudden load step but soon settles to the pre-set value 30 V. The system does not become unstable.

③ At $t = 0.15$ s, the converter enters the perfect DCM when the load is further changed to 47 Ω. As shown in FIGURES 3, the converter still operates stably and u_o keeps at the pre-set value.

To demonstrate the superior performances of the IEBC method, compared with the SEBC method and a

TABLE 1. Simulation comparison results under cases of load and input voltage variations.

Disturbance (R or u_{in})	IEBC		SEBC		PID controller	
	Δu_o(V)	$t_{settling}$(ms)	Δu_o(V)	$t_{settling}$(ms)	Δu_o(V)	$t_{settling}$(ms)
10 Ω → 27 Ω	0.8	4	0.8	7	2.2	13
27 Ω → 47 Ω	0.1	2	0.02	4	0.8	10
47 Ω → 10 Ω	-0.8	3	-0.8	4	-2.5	15
15 V → 18 V	0.4	2	0.4	3	0.8	8
18 V → 15 V	-0.4	2	-0.4	4	-0.8	10

TABLE 2. The simulation results of u_o and Δu_{steady} with the SEBC under various operation conditions.

Operation conditions (u_{in}/R)	15 V/10 Ω	15 V/27 Ω	15 V/47 Ω	18 V/10 Ω
u_o (V)	28.6	29.1	29.2	29
Δu_{steady} (V)	1.4	0.9	0.8	1.0

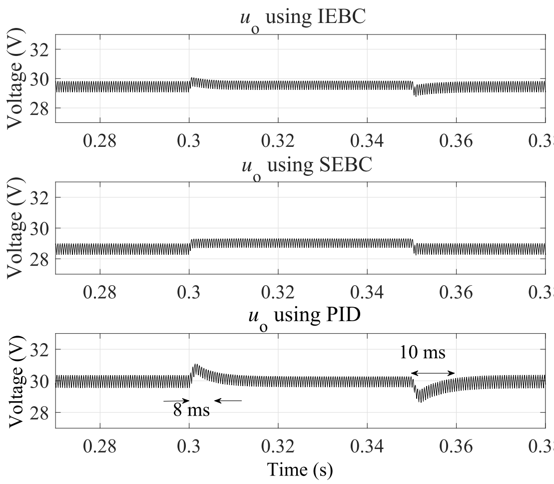

FIGURE 5. The simulation results of the responses of u_o to input voltage variations (15 V → 18 V → 15 V).

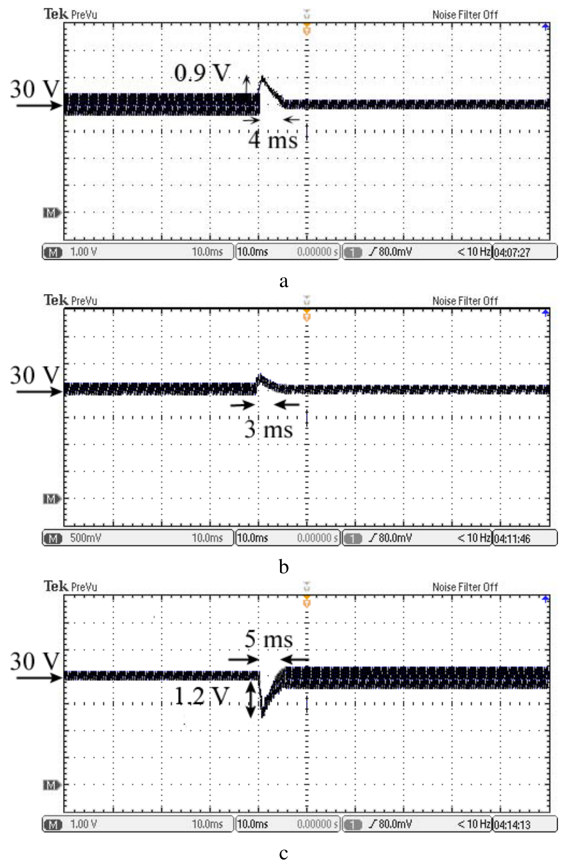

FIGURE 6. The experimental rusults of the responses of u_o using the proposed IEBC to load step changes. a: From 10 Ω to 27 Ω; b: From 27 Ω to 47 Ω; c: From 47 Ω to 10 Ω.

current-mode PID controller, the responses to load and input voltage disturbances of the converter are discussed as follows. By using the SISO tool box in MATLAB, the PID controller is established with the 382 Hz cross-over frequency and the 54.5 degrees phase margin. Step changes in loads, which is 10 Ω → 27 Ω → 47 Ω, are applied. At $t = 0.22$ s, the load is changed back to 10 Ω. Then step changes in the input voltage as 15 V → 18 V → 15 V are applied. FIGURES 4 and 5 show the responses of the converter to such load and input voltage step changes. The results demonstrate that, compared with the PID, the voltage peak overshoot Δu_o is reduced from 2.2 V (using the PID) to 0.8 V (using the IEBC) under the case that the load steps from 10 Ω to 27 Ω. And the settling time $t_{settling}$ is shortened to 4 ms (using the IEBC) from 13 ms (using the PID). These comparison results of the responses are summarized in TABLE 1, which shows that, compared with that of the PID, Δu_o of the IEBC is significantly reduced and $t_{settling}$ of the IEBC are significantly shortened.

Meanwhile, from FIGURES 4 and 5, it reveal that, under various operation conditions, u_o using the SEBC cannot settle to the pre-set value but has certain steady-state errors Δu_{steady} after reaching steady states. For example, under operation conditions of $R = 10$ Ω, u_o has the steady-state errors as 1.6 V to the pre-set value 30 V. TABLE 2 summarizes the steady-state value of u_o and the steady-state errors Δu_{steady} using the SEBC under various operation conditions. In contrast, the results in FIGURES 4 and 5 demonstrate that, there are no steady-state errors in u_o using the IEBC because of the function of the PI voltage controller.

B. EXPERIMENTAL COMPARISON RESULTS

Based on a dSPACE DS1104, an experimental boost converter prototype is constructed. The current and voltage are

TABLE 3. Experimental comparison results under cases of load and input voltage variations.

Disturbance (R or u_{in})	IEBC Δu_o(V)	IEBC t_{settling}(ms)	SEBC Δu_o(V)	SEBC t_{settling}(ms)	PID controller Δu_o(V)	PID controller t_{settling}(ms)
10 Ω → 27 Ω	0.9	4	0.8	16	2.2	13
27 Ω → 47 Ω	0.3	3	0.2	13	0.8	15
47 Ω → 10 Ω	-1.2	5	-1	11	-3.2	15
15 V → 18 V	0.5	4	0.4	14	0.8	8
18 V → 15 V	-0.4	3	-0.4	12	-1	8

TABLE 4. The experimental results of u_o and Δu_{steady} with the SEBC under various operation conditions.

Operation conditions (u_{in}/R)	15 V/10 Ω	15 V/27 Ω	15 V/47 Ω	18 V/10 Ω
u_o (V)	28.4	29.2	29.4	28.8
Δu_{steady} (V)	1.6	0.8	0.6	1.2

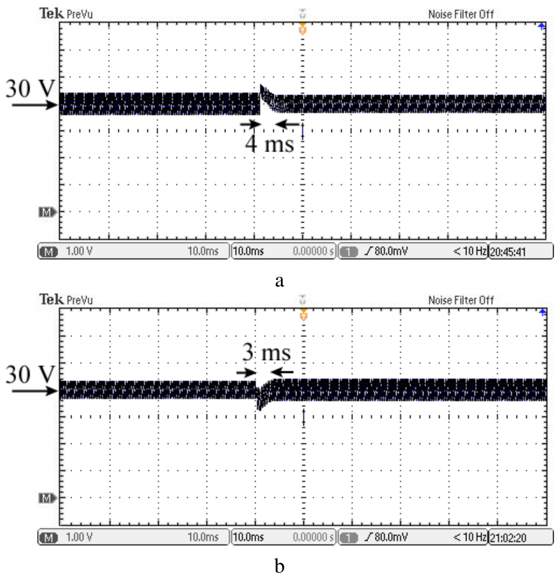

FIGURE 7. The experimental rusults of the responses of u_o using the proposed IEBC to input voltage variations. a: From 15 V to 18 V; b: From 18 V to 15 V.

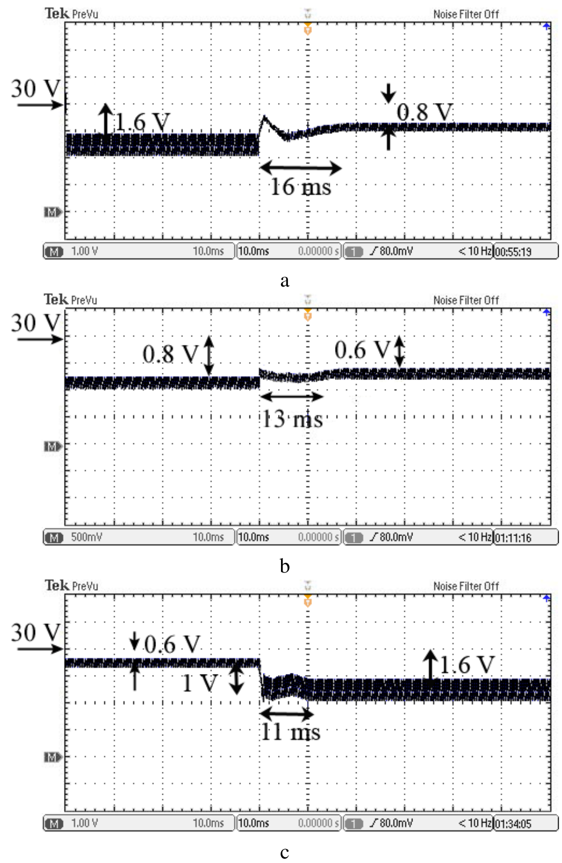

FIGURE 8. The experimental rusults of the responses of u_o using the SEBC to load step changes. a: From 10 Ω to 27 Ω; b: From 27 Ω to 47 Ω; c: From 47 Ω to 10 Ω.

measured by HALL sensors (CHV-25P and CHB-25NP/6A), respectively. The gate drivers of the IGBT are SKYPER 32R. The experimental results using the IEBC, the SEBC and the PID controllers are shown in FIGURES 6-11. In order to provide a intuitive and clear display of steady-state errors, the experiment tests are made under the disturbances in both loads and source voltages.

The comparative results of FIGURES 6-11 reveal the static performance under various operation conditions and the dynamic responses to load and input voltage step changes. TABLE 3 summarizes the comparison results of Δu_o and t_{settling} under all the dynamic cases. From FIGURES 6, 7, 10, 11 and TABLE 3, it is observed that the experiments get consistent results with the simulation, which show that Δu_o using the IEBC is significantly reduced and t_{settling} using the IEBC is significantly shorten compared with that of the PID controller. And from FIGURES 8 and 9, it is observed that although Δu_o using the SEBC is reduced and t_{settling} is shorten by comparing with that of the PID, yet there are certain steady-state errors Δu_{steady} after reaching steady states under various operation conditions. FIGURE 8a illustrate that u_o under operation conditions of $R = 10$ Ω and $R = 27$ Ω has steady-state errors as 1.6 V and 0.8 V to the pre-set value 30 V, respectively. The experimental results of u_o and Δu_{steady} using the SEBC under various operation conditions is summarized in TABLE 4. It is observed from TABLE 4 that, using the SEBC, steady-state errors are

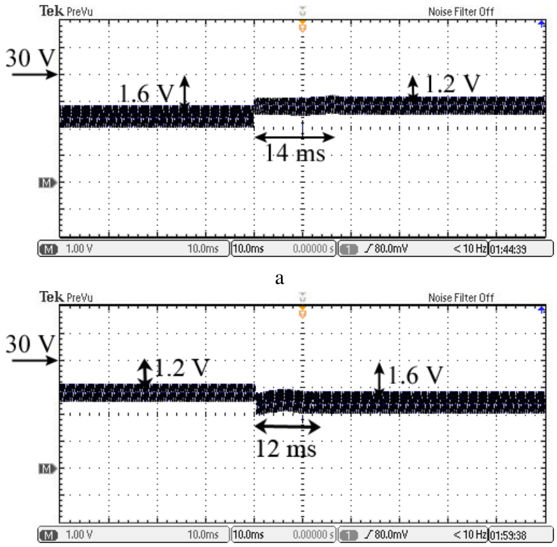

FIGURE 9. **The experimental rusults of the responses of u_o using the SEBC to input voltage variations. a: From 15 V to 18 V; b: From 18 V to 15 V.**

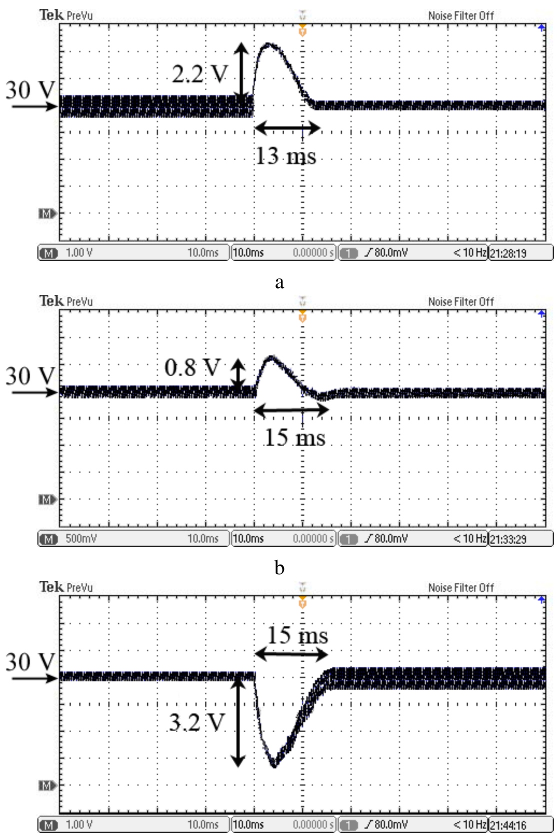

FIGURE 10. **The responses of u_o using the PID of the actual boost converter to load changes. a: From 10 Ω to 27 Ω; b: From 27 Ω to 47 Ω; c: From 47 Ω to 10 Ω.**

produced due to the neglection of circuit energy losses. The differences of Δu_{steady} under various operation conditions are due to the different value of the energy losses (mainly the energy loss of the inductor parasitic DC resistance).

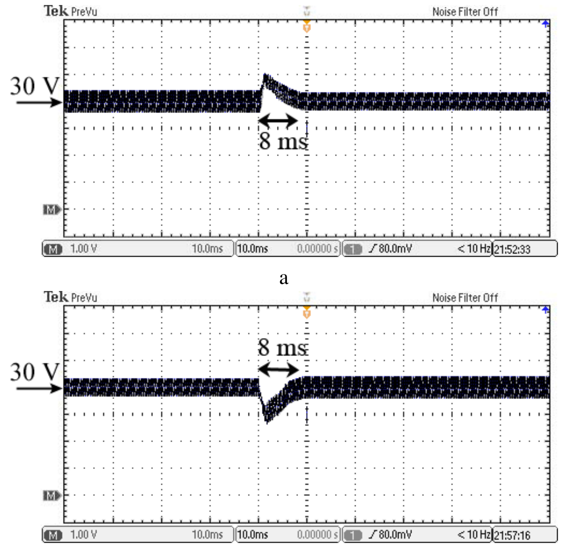

FIGURE 11. **The responses of u_o using the PID of the actual boost converter to input voltage variations. a: From 15 V to 18 V; b: From 18 V to 15 V.**

VI. CONCLUSION

In this research, the IEBC method has been proposed and implemented effectively for controlling boost converters. On the basis of the control principle of the previously developed control methods based on the conservation of energy in circuits, in the proposed control method, a PI voltage controller is added, as a result, the output voltage steady-state errors due to the neglection of circuit energy losses is removed. Furthermore, the stability of the converter controlled by the IEBC has been proved using Routh-Hurwitz criterion.

Simulation and experimental results demonstrate the proposed IEBC method can settle the output voltage to a pre-set value though circuit energy losses are not considered. Meanwhile, the comparison to the PID controller reveals that the IEBC keeps the advantage of the previously developed control methods based on the conservation of energy in circuits, which is superior dynamic performance, in terms of smaller voltage shoots and shorter settling times under the step changes of input voltage and load current. These results demonstrate that, using the IEBC, accurate static and fast dynamic performances are achieved even though circuit energy losses are neglected due to the complexity in their measurement and calculation.

REFERENCES

[1] J. A. Morales-Saldaña, E. Palacios-Hernández, and R. Loera-Palomo, "Parameters selection criteria of proportional–integral controller for a quadratic buck converter," *IET Power Electron.*, vol. 7, no. 6, pp. 1527–1535, Jun. 2014.

[2] V. P. Arikatla and J. A. A. Qahouq, "Adaptive digital proportional–integral–derivative controller for power converters," *IET Power Electron.*, vol. 5, no. 3, pp. 341–348, Mar. 2012.

[3] A. Shyam and F. Daya J L, "A comparative study on the speed response of BLDC motor using conventional PI controller, anti-windup PI controller and fuzzy controller," in *Proc. Int. Conf. Control Commun. Comput. (ICCC)*, Dec. 2013, pp. 68–73.

[4] G. S. John and A. T. Vijayan, "Anti-windup PI controller for speed control of brushless DC motor," in *Proc. IEEE Int. Conf. Power, Control, Signals Instrum. Eng. (ICPCSI)*, Sep. 2017, pp. 1068–1073.

[5] S. C. Huerta, A. Soto, P. Alou, J. A. Oliver, O. Garcia, and J. A. Cobos, "Advanced control for very fast DC–DC converters based on hysteresis of the C_{out} current," *IEEE Trans. Circuits Syst. I, Reg. Papers*, vol. 60, no. 4, pp. 1052–1061, Apr. 2013.

[6] L. Gil-Antonio, B. Saldivar, O. Portillo-Rodriguez, G. Vazquez-Guzman, and S. M. De Oca-Armeaga, "Trajectory tracking control for a boost converter based on the differential flatness property," *IEEE Access*, vol. 7, pp. 63437–63446, 2019.

[7] J. Wu and Y. Lu, "Adaptive backstepping sliding mode control for boost converter with constant power load," *IEEE Access*, vol. 7, pp. 50797–50807, 2019.

[8] S. Huerta-Moro, J. I. Trujillo-Flores, J. C. Villegas-Hernandez, A. M. Rodriguez-Domingez, J. F. Guerrero-Castellanos, and V. R. Gonzalez-Diaz, "A simple sliding-mode control circuit for buck DC-DC converters," in *Proc. IEEE Int. Fall Meeting Commun. Comput. (ROC&C)*, Mar. 2019, pp. 24–27.

[9] T. Gao, S. Zhang, S. Zhang, and J. Zhao, "A dynamic model and modified one-cycle control of three-level front-end rectifier for neutral point voltage balance," *IEEE Access*, vol. 5, pp. 2000–2010, 2017.

[10] D. Murillo-Yarce, J. Munoz, and C. Restrepo, "Mamdani type PI-fuzzy controller in a boost converter," in *Proc. IEEE Int. Conf. Ind. Technol. (ICIT)*, Feb. 2020, pp. 487–492.

[11] R. J. Atmur, "Rule-based balanced energy controller," in *Proc. Amer. Control Conf.*, San Diego, CA, USA, Aug. 1999, pp. 1673–1676.

[12] J. Chavarria, D. Biel, F. Guinjoan, C. Meza, and J. J. Negroni, "Energy-balance control of PV cascaded multilevel grid-connected inverters under level-shifted and phase-shifted PWMs," *IEEE Trans. Ind. Electron.*, vol. 60, no. 1, pp. 98–111, Jan. 2013.

[13] Y. Sun, Z. Ding, and H. Wang, "Energy-balancing-based control design for power systems," in *Proc. 10th World Congr. Intell. Control Autom.*, Jul. 2012, pp. 2364–2369.

[14] S. Janjornmanit, C. Dechthummarong, and S. Panta, "Active power filter designed by energy balancing control," in *Proc. 1ST IEEE Conf. Ind. Electron. Appl.*, May 2006, pp. 1–4.

[15] W. Wei, Z. Sun, H. Song, H. Wang, X. Fan, and X. Chen, "Energy balance-based steerable arguments coverage method in WSNs," *IEEE Access*, vol. 6, pp. 33766–33773, 2018.

[16] C. Verdugo, J. I. Candela, and P. Rodriguez, "Energy balancing with wide range of operation in the isolated multi-modular converter," *IEEE Access*, vol. 8, pp. 84479–84489, 2020.

[17] P. Gupta and A. Patra, "Energy based switching control scheme for DC–DC buck-boost converter circuits," in *Proc. Int. Conf. Power Electron. Drives Syst.*, Nov. 2005, pp. 1525–1529.

[18] A. Patra and P. Gupta, "Hybrid mode-switched control of DC–DC boost converter circui," *IEEE Trans. Circuits Syst. II, Exp. Briefs*, vol. 52, no. 11, pp. 734–738, Nov. 2002.

[19] J. Kaczmarek and A. Mazurek, "Comparison of classic DC/DC converters with converters equipped with analog-digital regulator based on law of conservation of energy (Bumblebee Type)," in *Proc. 14th Int. Conf. Mixed Design Integr. Circuits Syst.*, Jun. 2007, pp. 564–569.

[20] J. Kaczmarek and A. Mazurek, "New concept of DC/DC converters digital control based on law of conservation of energy–project 'Bumblebee"," in *Proc. 14th Int. Conf. Mixed Design Integr. Circuits Syst.*, Jun. 2007, pp. 586–591.

[21] L. Wang, Q. H. Wu, Y. K. Tao, and W. H. Tang, "Switching control of buck converter based on energy conservation principle," *IEEE Trans. Control Syst. Technol.*, vol. 24, no. 5, pp. 1779–1787, Sep. 2016.

[22] L. Wang, Q. H. Wu, W. H. Tang, B. Li, and Z. X. Xu, "Energy balance analysis and control for boost converters," in *Proc. 43rd Annu. Conf. IEEE Ind. Electron. Soc. IECON*, Oct. 2017, pp. 8194–8200.

[23] K. Ogata, *Modern Control Engineering*. Englewood Cliffs, NJ, USA: Prentice-Hall, 2001.

LEI WANG (Member, IEEE) received the B.Eng. and M.Sc. degrees in electrical engineering from Chongqing University, Chongqing, China, in 2008 and 2011, respectively, and the Ph.D. degree in electrical engineering from the South China University of Technology, Guangzhou, China, in 2016. She is currently holding a postdoctoral position with the School of Electric Power Engineering, South China University of Technology. Her research interests include renewable energy integration in power grids, modeling and control of power converters, and non-linear analysis of power electronics.

QINGHUA WU received the Ph.D. degree in electrical engineering from The Queens University of Belfast (QUB), Belfast, U.K., in 1987. From 1987 to 1991, he was a Research Fellow and a Senior Research Fellow with QUB. He joined the Department of Mathematical Sciences, Loughborough University, U.K., in 1991, as a Lecturer. He was appointed a Senior Lecturer with Loughborough University. He joined The University of Liverpool, Liverpool, U.K., in September 1995, to take up his appointment to the Chair of electrical engineering with the Department of Electrical Engineering and Electronics. He is currently a Distinguished Professor with the School of Electric Power Engineering, South China University of Technology, Guangzhou, China, and the Director of the Energy Research Institute of the University. He has authored or coauthored more than 440 technical publications, including 240 journal articles, 20 book chapters, and three research monographs published by Springer. His research interests include nonlinear adaptive control, mathematical morphology, evolutionary computation, power quality, and power system control and operation. He is a Fellow of IET and InstMC. He is also a Chartered Engineer.

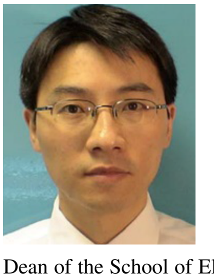

WENHU TANG (Senior Member, IEEE) received the B.Eng. and M.Sc. degrees in electrical engineering from the Huazhong University of Science and Technology, Wuhan, China, in 1996 and 2000, respectively, and the Ph.D. degree in electrical engineering from the University of Liverpool, Liverpool, U.K., in 2004. From 2004 to 2013, he was a Postdoctoral Research Associate and a Lecturer with the University of Liverpool. He is currently a Distinguished Professor and the Vice Dean of the School of Electric Power Engineering, South China University of Technology, Guangzhou, China. He has authored or coauthored more than 100 research articles, including 40 journal articles and one Springer research monograph. His research interests include renewable energy integration in power grids, condition monitoring and fault diagnosis for power apparatus, multiple criteria evaluation, and intelligent decision support systems.